RivWidth: A Software Tool for the Calculation of River Widths From Remotely Sensed Imagery

Tamlin M. Pavelsky and Laurence C. Smith

***Abstract*—RivWidth is an implementation in ITT Visual Information Solutions IDL of a new algorithm that automates the calculation of river widths using raster-based classifications of inundation extent derived from remotely sensed imagery. The algorithm utilizes techniques of boundary definition to extract a river centerline, derives a line segment that is orthogonal to this line at each centerline pixel, and then computes the total river width along each orthogonal. The output of RivWidth is comparable in quality to measurements derived using manual techniques; yet, it continuously generates thousands of width values along an entire stream course, even in multichannel river systems. Uncertainty in RivWidth principally depends on the quality of the water classification used as an input, though pixel resolution and the values of input parameters play lesser roles. Source code for RivWidth can be obtained by visiting http://pavelsky.googlepages.com/rivwidth.**

***Index Terms*—Algorithms, fluvial geomorphology, hydrology, rivers, river width.**

I. Introduction

RIVER flow width (w) is a critical parameter in a wide variety of hydrologic applications. It is measured as the shortest cross-sectional distance from water's edge to water's edge, orthogonal to the river channel. Flow widths vary constantly with discharge and, as such, differ from channel widths (i.e., bank-to-bank width). Most notably, it is one of three fundamental hydraulic variables, together with depth (d) and velocity (v), whose product determines the river discharge Q (i.e., $Q = wdv$) [1]. Furthermore, each of these variables exhibits a power law relationship with Q (i.e., $w = aQ^b$, $d = cQ^e$, and $v = fQ^g$, where a, b, c, e, f, and g are empirically derived constants) that, in theory, enables Q to be estimated from any one of these three variables if the empirical constants are known. The width is also central to the calculation of the hydraulic radius R, which is a key term in the empirical Manning and Chezy hydraulic formulations for the calculation of stream flows in the absence of flow data [2]. Moreover, the channel width plays a role in physical and biological processes in and around rivers, including erosion and sediment transport [3], [4], river ecology [5], [6], and human use, such as site selection for bridges and dams.

With the advent of satellite remote sensing, it has become increasingly possible to estimate useful hydraulic parameters, most notably the river discharge Q, from space [7], [8]. Of the three principal elements of discharge measurement (width, depth, and velocity), the width is perhaps the most readily measured using currently available remotely sensed imagery [9]. Recent studies have successfully demonstrated the feasibility of using remotely sensed changes in width to estimate the river flow in a variety of environments [10]–[15].

Although it is theoretically possible to calculate such width values manually, it becomes impractical if hundreds or thousands of river width values must be obtained. As a result, an automated method for continuously extracting river width values from raster-based imagery would prove valuable in many hydrologic studies. The purpose of this letter is to present RivWidth, a new software tool written in the ITT Visual Information Solutions (ITTVIS) IDL programming language that automates the continuous extraction of river width values at regular intervals along an entire river course.

II. Methods

Broadly speaking, the algorithm used by RivWidth to calculate river width values can be divided into two steps: 1) derivation of a centerline down the river and 2) calculation of the width at each pixel along that centerline. After a discussion of the required inputs to RivWidth, each of these phases will be examined in detail. A thorough examination of errors in RivWidth is presented in Section III. Examples are presented for a large highly anastomosing river in Eastern Siberia (Lena River) and a large predominantly single-channel river in the Eastern U.S. (Ohio River). For a more detailed discussion of algorithms used in this study, as well as the IDL source code for RivWidth, please see supporting online material available at http://pavelsky.googlepages.com/rivwidth.

A. Inputs to RivWidth

Only two initial inputs are required by RivWidth. The first is a binary mask that assigns water pixels a value of 1 and nonwater pixels a value of 0 [Figs. 1(a) and 2(a)]. This is referred to as the channel mask, since it shows all of a river's various channels and islands. The second input is another binary mask that differentiates those areas that are within the river boundary (including islands) and those areas outside the river boundary [Figs. 1(b) and 2(b)]. This input is referred to as the river mask. Note that these two products may be identical for a river lacking islands. Numerous methods exist for the classification of imagery and the extraction of water masks suitable for input to RivWidth [16], [17], though the details of such techniques are beyond the scope of this letter.

The provided examples use two different rivers and data sources. The first uses channel and river masks derived from

Manuscript received March 6, 2007; revised May 25, 2007. This work was supported by the National Aeronautics and Space Administration through the Terrestrial Hydrology Program under Grant NNG06GE05G.

The authors are with the Department of Geography, University of California, Los Angeles, Los Angeles, CA 90095-1524 USA (e-mail: pavelsky@ucla.edu; lsmith@geog.ucla.edu).

Digital Object Identifier 10.1109/LGRS.2007.908305

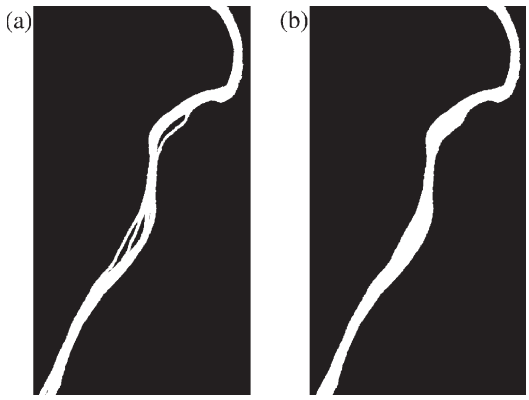

Fig. 1. Required inputs to RivWidth are a channel mask (a) and a river mask (b) shown here for the Ohio River.

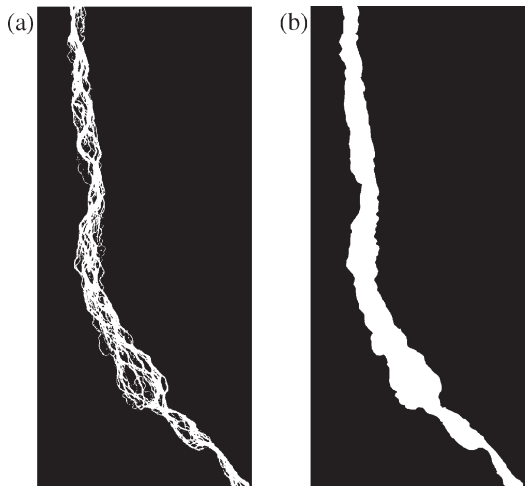

Fig. 2. Required inputs to RivWidth are a channel mask (a) and a river mask (b) shown here for the Lena River.

the 250-m Moderate Resolution Imaging Spectroradiometer (MODIS) band 2 (near-infrared, 0.841–0.876 μm) over the Lena River, with a simple threshold used to differentiate water from nonwater pixels. The second uses channel and river masks of the Ohio River, which were extracted from the U.S. Geological Survey National Land Cover Dataset—a raster land-cover classification derived from 30-m Landsat Thematic Mapper imagery [18].

B. Delineating a Centerline

The first step in continuously extracting river widths along a reach is the calculation of a centerline for the river. The delineation of this line is essential because all calculations of the river widths must be made perpendicularly to the direction of flow, which is approximated by the centerline. The method used to derive the centerline is based upon techniques of edge detection and boundary definition commonly utilized in computer vision and image-processing applications [19]. Two representative techniques of edge detection were developed by Marr and Hildreth [20] and Canny [21]. Each of these algorithms is based around three fundamental steps: 1) convolution of an image with a Gaussian smoothing filter to eliminate high-frequency noise; 2) convolution of the smoothed image with one or more Laplacian filters to compute either maxima in the first derivative (Canny) or zero-crossings in the second derivative (Marr–Hildreth); and 3) extraction of an edge map from the resulting image. In addition to the number of Laplacian filters used, the techniques principally differ in the third step, where Marr and Hildreth use a simple threshold to extract edges from the surrounding image, whereas Canny employs a dual-threshold technique in which a preliminary set of edges is defined using one threshold, and then, a lower threshold is used to fill in gaps in these edges. To calculate a centerline, we utilize a method similar to the Marr–Hildreth technique because it is less computationally intensive than the Canny edge detector while being equally effective in relatively noise-free images such as those used here [19].

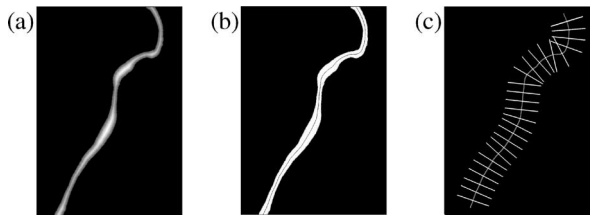

Fig. 3. Examples of intermediate processing outputs from RivWidth for the Ohio River. (a) Map of distance from each river pixel to the nearest nonriver pixel, (b) convolution of (a) with a Laplacian mask, and (c) derived river centerline and the orthogonal lines along which river width is calculated. For clarity, the orthogonals in (c) are only included for every 40th pixel.

The algorithm that is used to calculate a centerline starts with the binary river mask [Figs. 1(b) and 2(b)] and determines the distance from each river pixel to the nearest nonriver pixel using a uniform-cost search algorithm [22] [Figs. 3(a) and 4(a)]. In many cases, this step is the most computationally intensive portion of RivWidth because it is often necessary to search a large number of pixels to ensure an accurate minimum distance value. For the 701×1001 pixel mask of the Ohio River [Fig. 2(b)], the calculation required 57 min on a dual-core Pentium 4 workstation with 2 GB of random access memory. Because there are no rapid changes in the values between adjacent pixels in this distance map, it is unnecessary to apply a smoothing filter before further processing.

The distance map is then convolved with a bidirectional Laplacian filter in a manner similar to the Marr–Hildreth edge detection algorithm [20]. Convolution with a Laplacian filter of this type can be thought of as calculating the second derivative of an image, with regions of rapidly changing pixel value having high output values and uniform regions having low output values. Therefore, along a "ridge" of high distance values occurring at the center of the river, Laplacian values are close to zero because distance values on either side of the central pixel are often nearly identical [Figs. 3(b) and 4(b)]. To obtain an initial centerline, a threshold between 0.7 and 0.9 is applied to the output of the Laplacian convolution, with anything below this value considered part of the centerline. Within these bounds, the threshold value has little impact on the final width values but can be important in ensuring the continuity of the centerline, with a higher value resulting in a more robust centerline calculation.

A normal problem is that the derived centerline may be more than one pixel wide—a problem exacerbated by a high threshold value. The most frequent cause is an even number of pixels

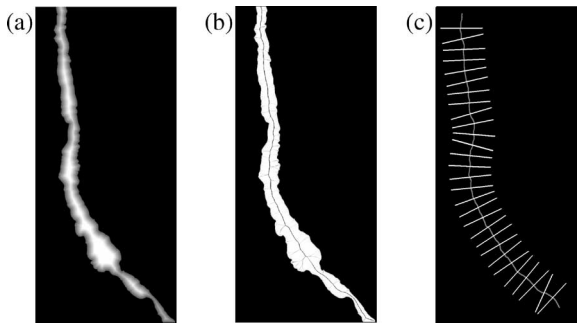

Fig. 4. Examples of intermediate processing outputs from RivWidth for the Lena River. (a) Map of distance from each river pixel to the nearest non-river pixel, (b) convolution of (a) with a Laplacian mask, and (c) derived river centerline and the orthogonal lines along which river width is calculated. For clarity, the orthogonals in (c) are only included for every 40th pixel.

in a river cross section, resulting in two central pixels with nearly identical distances from the edge of the river. To solve this problem, a breadth-first search algorithm is used to extract the shortest path along the initial centerline between pixels at either end of the desired river reach [22]. The resulting output, which is a sequence of adjacent pixels running between the two input points, is the final centerline and the appropriate input for the actual calculation of the river width [Figs. 3(c) and 4(c)].

C. Calculating the River Width

In RivWidth, the river width is calculated along a series of transects that are orthogonal to the centerline at each centerline pixel. To obtain these orthogonals, we begin with two user-inputted length values (segments AB and CD in Fig. 5), which remain constant for all orthogonals calculated along a centerline. The lengths of AB used in defining orthogonals for the Ohio River and Lena River (Figs. 3 and 4) were 1500 and 12 500 m, respectively, whereas the lengths of segment CD were 2400 and 20 000 m. For each pixel A in the centerline, the locations of pixels C and D on the centerline are determined such that the lengths of AC and AD are equal. Because we know the lengths of AB, AC, and AD, we can compute the lengths of BC and BD using simple trigonometry. Employing a simple iterative search, we determine the location of pixel B at which the lengths of BC and BD most closely converge and at which the length of AB matches the user-specified length value. We then use the same process to determine the location of pixel E on the opposite side of the river channel. These two pixels, B and E, define the orthogonal line along which width at pixel A will be calculated [Figs. 3(c) and 4(c)]. In cases where one of the endpoints of the orthogonal lies outside the image bounds, no width value is calculated by RivWidth.

The actual calculation of the river width is performed for each centerline pixel using the series of pixel values that intersect its orthogonal line segment. In a single-channel river, the river width is simply calculated as the Euclidian distance between the centers of the two pixels in the channel mask at which the orthogonal intersects the riverbank. In multichannel rivers, the Euclidian distance across each channel is separately measured, and the resulting values are summed up to provide the final value of the river width. RivWidth provides two final outputs: 1) a new image with a width value assigned to each pixel along the centerline and 2) a comma-separated text file containing the coordinates of each centerline pixel and the corresponding value for the river width. RivWidth also has the capability of computing the mean width for reaches of a user-defined length. This is accomplished simply by averaging individual river width values along centerline segments of equal length and then assigning the average value to the centerline pixel at the center of each segment.

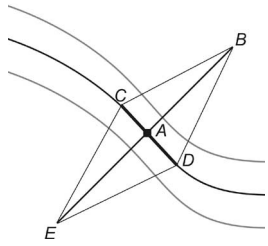

Fig. 5. Schematic showing method used to derive an orthogonal to the centerline at pixel A. Segments CD and AE are orthogonal, and the lengths of CD and AB are parameters defined by the user.

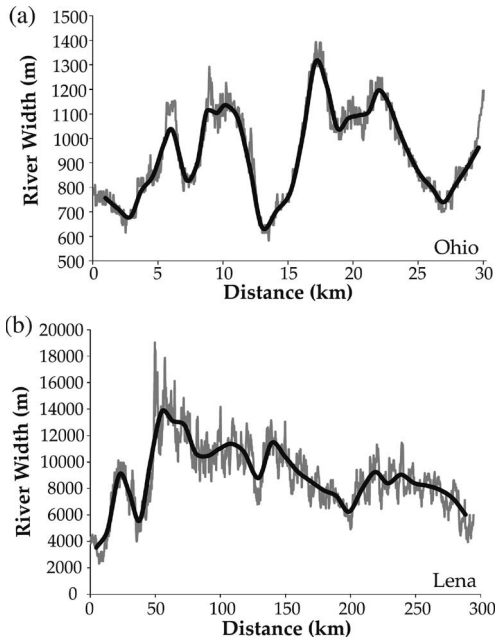

Fig. 6. Width profiles for the portions of (a) the Ohio River and (b) the Lena River shown in Figs. 1 and 2. The bold lines represent widths averaged using a filter of 32 pixels (Ohio) and 38 pixels (Lena), the approximate mean widths of the two rivers. These width values match closely with values manually measured from Figs. 1(a) and 2(a).

III. Results and Discussion

RivWidth successfully calculates width values for both single-channel and complex-river-channel configurations. The Ohio River [Fig. 6(a)] has a simple-channel structure, whereas the portion of the Lena River [Fig. 6(b)] examined here is highly anastomosing. As such, it is not surprising that the Lena River shows more high-frequency variability in width than does the Ohio River. In each case, averaging the width using a window equal in length as the mean river width (945 m for the Ohio River and 8747 m for the Lena River) removes much of this variability, resulting in a relatively smooth river width profile.

TABLE I
VARIATIONS IN MEAN WIDTH AND STANDARD DEVIATION OF WIDTH VALUES ON THE PORTION OF THE OHIO RIVER SHOWN IN FIG. 1 RESAMPLED TO FOUR DIFFERENT SPATIAL RESOLUTIONS

Resolution	Mean Width (m)	St. Dev. (m)
30 m	939	175
60 m	936	179
90 m	940	178
120 m	940	186

We assessed the accuracy of RivWidth by: 1) comparing selected output values with manually measured widths obtained using the measurement tool in ITTVIS ENVI; 2) conducting a sensitivity analysis of the width's response to changes in input parameters; and 3) comparing width values for the same river reach using imagery with different pixel resolutions. Evenly spaced cross sections 40 pixels apart were selected for both the Ohio River ($n = 24$) and the Lena River ($n = 29$) [Figs. 3(c) and 4(c)], and the river width was measured along the same orthogonal line segment used by RivWidth. The average difference between the manually measured distance and the output of RivWidth is 12 m for the Ohio River (pixel resolution = 30 m and mean width = 939 m) and 180 m for the Lena River (pixel resolution = 250 m and mean width = 8747 m), suggesting that RivWidth closely matches careful manual measurement techniques.

We also tested the sensitivity of mean river width values on the Ohio River to variations in the length of the line segments used in the calculation of orthogonals to the centerline (AB and CD in Fig. 5). So long as segment CD is at least as long as half the mean channel width, sensitivity is quite low, with variations of less than 1% in mean width (450–2130 m segments tested: average mean width = 939 m and standard deviation = 1 m). A similar result was found for the variation in AB, so long as AB is long enough to encompass the entire river width in all cases (900–3000 m segments tested: average mean width = 938 m and standard deviation = 1 m).

Given the relatively low uncertainty associated with the variation in these input parameters, the principal determinants of the error in RivWidth are the quality and spatial resolution of the channel mask. An unreliable water classification will result in higher rates of error, whereas a high-accuracy mask will provide accurate width measurements. The spatial resolution of the original imagery from which the channel mask is derived also affects the level of error in the width values, with the use of lower resolution products generally resulting in higher uncertainty. Assuming an accurate input classification, the maximum uncertainty associated with the boundary effects in the width calculations can be calculated using the following equation:

$$E = 1/2RC$$

where E is the uncertainty, R is the pixel resolution, and C represents the number of riverbanks crossed by the orthogonal segment along which the width is calculated. As such, uncertainty increases with an increasing number of river channels. The effect of decreasing spatial resolution in a single-channel river was tested by resampling the 30-m Ohio River masks shown in Fig. 1 to 60-, 90-, and 120-m resolution and calculating the width using each new mask (Table I). In this case, results suggest a minimal change in mean width with decreasing resolution, though the standard deviation of width values does increase somewhat.

ACKNOWLEDGMENT

The authors would like to thank D. Alsdorf and B. Kiel for their assistance with data and testing and three anonymous reviewers for their constructive comments.

REFERENCES

[1] L. Leopold and T. Maddock, The hydraulic geometry of stream channels and some physiographic implications, 1953. U.S. Geological Survey Professional Paper 252.
[2] D. Maidment, ed., *Handbook of Hydrology*. New York: McGraw-Hill, 1993.
[3] D. Knighton, *Fluvial Forms and Processes: A New Perspective*. London, U.K.: Arnold, 1998.
[4] M. Madej and V. Ozaki, "Channel response to sediment wave propagation and movement, Redwood Creek, CA, USA," *Earth Surf. Processes Landf.*, vol. 21, no. 10, pp. 17–38, Oct. 1996.
[5] F. Hayes and J. Sewlal, "The Amazon river as a dispersal barrier to passerine birds: Effects of river width, habitat and taxonomy," *J. Biogeogr.*, vol. 31, no. 11, pp. 1809–1818, Nov. 2004.
[6] J. Kemp, D. Harper, and G. Crosa, "Use of 'functional habitats' to link ecology with morphology and hydrology in river rehabilitation," *Aquat. Conserv.: Marine Freshwater Ecosystems*, vol. 9, no. 1, pp. 159–178, 1999.
[7] D. Alsdorf and D. Lettenmaier, "Tracking fresh water from space," *Science*, vol. 301, no. 5639, pp. 1491–1494, Sep. 2003.
[8] L. C. Smith, "Satellite remote sensing of river inundation area, stage, and discharge: A review," *Hydrol. Process.*, vol. 11, no. 10, pp. 1427–1439, Aug. 1997.
[9] D. Bjerklie, S. Dingman, C. Vorosmarty, C. Bolster, and R. Congalton, "Evaluating the potential for measuring river discharge from space," *J. Hydrol.*, vol. 278, no. 1, pp. 17–38, Jul. 2003.
[10] P. Ashmore and E. Sauks, "Prediction of discharge from water surface width in a braided river with implications for at-a-station hydraulic geometry," *Water Resour. Res.*, vol. 42, 2006. Art. W03406.
[11] G. Brackenridge, S. Nghiem, E. Anderson, and S. Chien, "Space-based measurement of river runoff," *EOS Trans. Amer. Geophys. Union*, vol. 86, no. 19, pp. 185–188, 2005.
[12] L. C. Smith, B. Isacks, R. Forster, A. Bloom, and I. Preuss, "Estimation of discharge from braided glacial rivers using ERS-1 SAR: First results," *Water Resour. Res.*, vol. 31, no. 5, pp. 1325–1329, 1995.
[13] L. C. Smith, B. Isacks, A. Bloom, and A. Murray, "Estimation of discharge from three braided rivers using synthetic aperture radar (SAR) satellite imagery: Potential applications to ungaged basins," *Water Resour. Res.*, vol. 32, no. 7, pp. 2021–2034, 1996.
[14] P. Townsend and J. Foster, "A synthetic aperture radar-based model to assess historical changes in lowland floodplain hydroperiod," *Water Resour. Res.*, vol. 38, no. 7, pp. 20–21, Jul. 2002. Art. No. 1115.
[15] K. Xu, J. Zhang, M. Watanabe, and C. Sun, "Estimating river discharge from very high-resolution satellite data: A case study in the Yangtze River, China," *Hydrol. Process.*, vol. 18, no. 10, pp. 1927–1939, Jul. 2004.
[16] R. Schowengerdt, *Remote Sensing: Models and Methods for Image Processing*, 2nd ed. San Diego, CA: Academic, 1997.
[17] M. J. Canty, *Image Analysis, Classification, and Change Detection in Remote Sensing: With Algorithms for ENVI/IDL*. Boca Raton, FL: CRC Press, 2006.
[18] *National Land Cover Dataset*, 1992, USGS Land Cover Institute. [Online]. Available: http://landcover.usgs.gov/prodescription.php
[19] D. Ziou and S. Tabbone, "Edge detection techniques an overview," *Int. J. Pattern Recogn. Image Anal.*, vol. 8, no. 4, pp. 537–559, 1998.
[20] D. Marr and E. Hildreth, "Theory of edge detection," *Proc. R. Soc. Lond., B Biol. Sci.*, vol. 207, no. 1167, pp. 187–217, 1980.
[21] J. Canny, "A computational approach to edge detection," *IEEE Trans. Pattern Anal. Mach. Intell.*, vol. 8, no. 6, pp. 679–714, Nov. 1986.
[22] T. Cormen, C. Leiserson, R. Sivest, and C. Stein, *Introduction to Algorithms*, 2nd ed. Cambridge, U.K.: MIT Press, 2001.